LAWRENCE
LIVERMORE
NATIONAL
LABORATORY

LLNL-JRNL-732604

Efficient method for the measurement of lifetime optical damage performance of thin film coatings from laser damage size analysis

S. Elhadj, J. Yoo

June 7, 2017

Optics Letters

Disclaimer

LLNL-JRNL-732604

Efficient method for the measurement of lifetime optical damage performance of thin film coatings from laser damage size analysis

Selim Elhadj* and Jae Hyuck Yoo

Physical and Life Sciences and NIF and Photon Sciences, Lawrence Livermore National Laboratory, 7000 East Avenue, Livermore, California 94550, USA

*Corresponding author: elhadj2@llnl.gov

Abstract

A laser damage test method based on damage size analysis (DSA) is described that simplifies the derivation of the lifetime optical damage threshold of film materials critical in the design of devices used in high-repetition-rate, high-power laser systems. The DSA method presented here is solely based on imaging to measure the damage site size produced from exposure to a known Gaussian-shaped beam with a fixed, systematically selected fluence well above the ablation threshold. The method locates the damage boundary produced from repeated exposures, using images with a high contrast, and maps it to the beam profile to extract a lifetime laser damage fluence threshold value. We validate the DSA approach using a few relevant transparent film material systems and by comparing it to the standard $S/1$ laser damage test method. The DSA method can be more efficient and accelerate materials development and validation necessary to support the design of high-power repetition-rated lasers and optoelectronic devices.

Optoelectronic devices used in high-power laser systems rely on materials evaluation from optical damage performance tests to establish limits and design parameters. The most susceptible materials are generally the thin films coatings with the lowest damage thresholds within the optical assembly [1], thus representing the failure point of a device when illuminated at peak fluences. For high-repetition-rate pulsed laser systems, the lifetime damage threshold is the most relevant performance criterium [2], if the optical and/or the electrical requirements of the films are also satisfied. Several standard methods are used for optical damage evaluation, including so-called $S/1$, $R/1$, and 1-on-1 damage tests [3,4].

S(N)/1 tests involve repeated (N) exposures at a single fluence level on a given test site. A range of fluence levels is then applied to an array of sites to determine a laser damage threshold. The $S/1$ laser damage probability curves as a function of fluence (for a given N) can be derived by counting the number of sites, where damage is observed and dividing by the total number of sites tested. The fluence where the onset of damage occurs represents an N-dependent damage threshold. Fluence (ϕ) dependent damage density data, $\rho(\phi)$, can also be used to derive a

measure of the material damage threshold [5,6]. For most materials, this approach requires rastering specialized large-aperture, high-power lasers that can probe large areas (>∼1 cm2) by exploiting the fluence spatial variability of the beam [7,8].

In general, laser damage test methods require examination of the site irradiated pre- and post-exposure, or the use of sensitive in-line diagnostics to capture subtle changes near the damage threshold [6,9]. This analysis can be time consuming and involves guessing and searching for a range of fluences to bracket the threshold and 100% damage probability. Thus, when the sample area is limited, reliable lifetime optical damage threshold assessments can become unpractical and, thus, cannot provide a measure of the maximum optical energy that an optical component can reliably be exposed during its lifetime use.

A simple laser lifetime damage test method presented here involves the spatial deconvolution of the laser beam spatial fluence map with the damage site map to extract a damage threshold value. The process is as follows. Effectively, a Gaussian-shaped beam is a beam with a high degree of fluence spatial contrast that is equivalent to multiple local fluence exposure levels produced from a single-pulse irradiation. Since the beam fluence, laser absorption, and resulting temperature rise and damage are directly mapped to the beam profile exposure, the damage threshold can be extracted from damage size analysis (DSA) of the damage site alone. The damage is intentionally produced with a peak axial fluence well above the film damage threshold, resulting in a damage site with a high imaging contrast to facilitate and improve automated image analysis. As described in Fig. 1A, in this pulsed train optical damage test embodiment, the easily identifiable and stable (not growing) boundary of the damage site separates the region of the film that is damaged from the region of the film that is not damaged [Fig. 1B]. The location of that boundary thus corresponds to the location of the threshold fluence on the fluence map, thereby enabling the determination of the lifetime damage threshold value, $F\mathrm{th}(N)$, where N is the number of exposures for a fixed fluence and site. This method is simple because, following pulse energy measurements, it only requires (1) determination of the beam diameter, $2w0$, which is derived here directly from a fit of the damage size data [10–13], and (2) image capture to measure the diameter, 2R, of the damage sites [Fig. 1C], and (3) systematically determining a single-pulse near-ablation fluence threshold, $F\mathrm{probe}$, to use as a fixed “probe” fluence level to carry out lifetime tests with N exposures [Fig. 1A]. Still, the observable damage itself need not involve any ablation at the threshold [14]. However, if $F\mathrm{probe}$ is too high, the stable damage site diameter quickly saturates with N to the value of the beam diameter, yielding no useful information on the threshold. If the fluence is too low, then the damage imaging contrast is limited, or requires too many exposures to clearly produce a sharp stable damage boundary contained within the beam footprint area. The reasons for the effectiveness of using such $F\mathrm{probe}$ will be discussed. The threshold, $F\mathrm{th}(N)$, can be determined for any number of pulse exposures, N, to derive a lifetime damage threshold that is suitable for a device expected usage of thin film materials, such as transparent electrodes addressed here for demonstration. In this Letter, multiple film material systems are laser damage tested by the standard $S(N)/1$ method and by the proposed DSA method for comparison to validate the DSA method. Most of the material systems tested are transparent and conductive, since they are potential candidates for high-power optoelectronics applications.

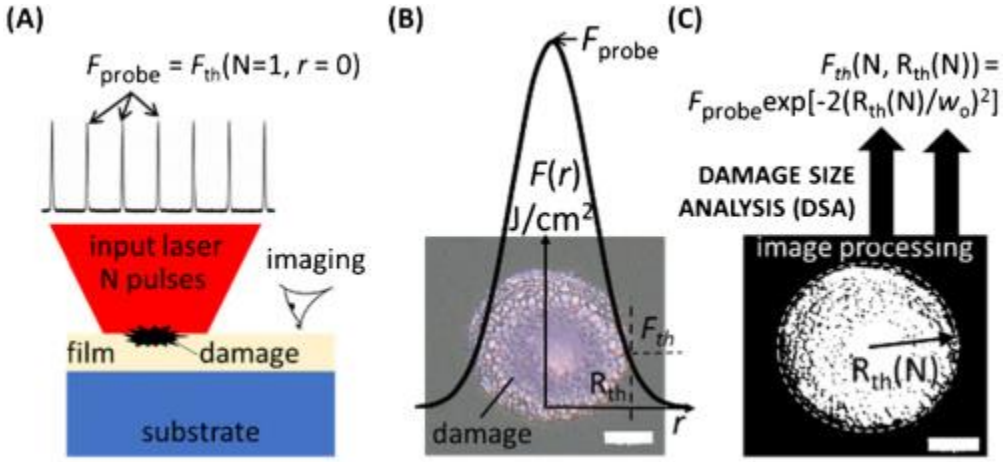

Fig. 1. (A) Illustration of the damage size analysis (DSA) method for the determination of lifetime optical damage threshold. Laser damage is produced from *N* pulsed exposures at a fixed fluence (*F*probe). In-line imaging is used for damage size measurements. (B) Illustrates a beam profile registered to a damage site with the fluence threshold (*F*th) taken at the edge of the site at the radial location *R*th. (C) *F*th(*N*) is calculated based on *R*th extracted from image analysis and knowledge of the beam radius, *w*0. White scale bars represent 20 μm in (B) and (C).

The analysis and experimental setup for the DSA measurements are described below. The laser damage setup consists of two stations: (1) a nanosecond-pulsed laser damage station and (2) a high-resolution monitoring station. Laser damage experiments were conducted in the damage station under ambient conditions using a Nd:YAG laser. The full width at half-maximum pulse duration was 7 ns at a wavelength of 1064 nm and at a repetition rate of 10 Hz. The power stability of the laser was estimated to be ~±3% over extended use. Laser pulses were focused by a single lens (focal length: 150 mm) and delivered to the film input surface at normal incidence. The laser pulse energy was adjusted using a thin film polarizer and a half-wave plate. The pick-off pulse energy was measured *in situ* using a beam splitter during damage tests to monitor the laser fluence. The calibrated ratio between the pick-off energy and energy delivered to the sample was measured and was used to derive the pulsed fluence levels delivered to the sample.

Pre- and post exposure, samples were translated to the imaging station with a two-axis linear stage (Planar DL, Aerotech), and images of damage sites were taken in transmission by a long working distance objective lens (Mitutoyo, NA: 0.42). Damage area was then obtained by automated image analysis using ImageJ and Python codes available in the Supplementary Materials (Code 1, Ref. [15], Code 2, Ref. [16], and Code 3, Ref. [17]). For *S*(*N*)/1 damage probability curves versus fluence, 10 separate sites were exposed at a given fluence, and the probability calculated as the number of sites that were damaged divided by 10. Bitmap post-exposure images were divided by exposure images to improve contrast.

The spatial distribution of the beam fluence profile determines the extent and, thus, the threshold of the damage site from *N*exposures. A recent report established this procedure for *N*=1 as a single “mono-shot” exposure laser damage test [18]. Extending this principle to a lifetime damage measurement method, the threshold fluence *F*th(*N*) is calculated from Gaussian beam profile with radius *w*0 given by where *R*th is the measured radius of the damage spot total area,

A, as Rth=√(A/π) from image analysis. The 1/e2 Gaussian beam radius can be determined from the slope of data fit of (2R)2 versus ln(F) for N=1, as indicated by Eq. (1), where F is the peak axial fluence of the beam (r=0) [10,12]. The w0 estimated using this data fitting agrees very well with independent measurements using a beam profiler to within less than 2% (data not shown). For a given film laser damage test, Fprobe(N=1) is determined by extrapolating the data fit above to its value at the vanishing damage site diameter [Fig. 2A]. As illustrated in Fig. 1B, the damage site at peak fluences above the ablation threshold represents mostly complete removal of the film up to the boundary of the damage site, making the imaging contrast simpler to analyze and the determination of Fprobe systematic.

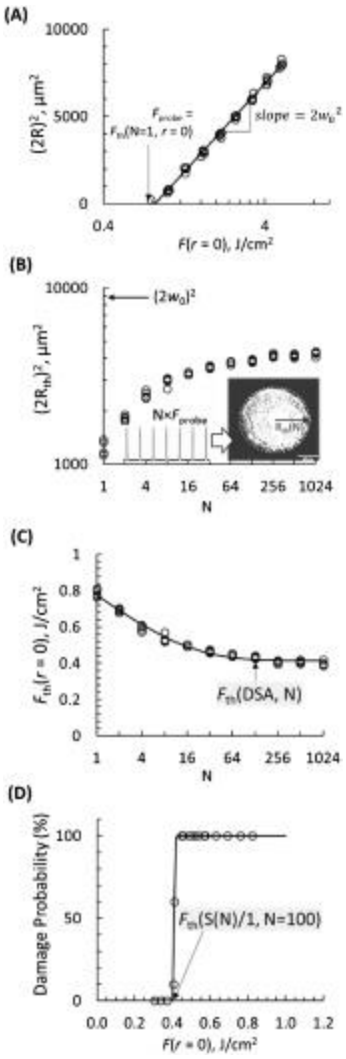

Fig. 2. (A) Representative fluence dependent laser ablation size data used to extrapolate a probe fluence, Fprobe, and 1/e2 beam radius, w0, on 20 nm thick Au film on a sapphire. (B) Damage size is determined for N exposures at a fixed Fprobe. (C) Size data in (B) are converted to Fth(N) threshold values using Eq. (1). (D) Fth(N=100) damage probability curve is derived for the same film using the S(N)/1 method. In (C) and (D) solid lines are semi-empirical fit of the data as described in the text. In (A)–(C) measurements were replicated 5 times.

In Fig. 2B, using $N\times F$probe repeated exposures, the size of the damage site increases with N until it ceases to increase. This stable damage boundary represents the location where the fluence is at the threshold of the film. Thus, beyond this location, the fluences are too low to produce any apparent damage. The beam area $(2w0)2$ indicated in Fig. 2B is significantly larger than the final saturation damage size, confirming that $2R\text{th}(N\rightarrow\infty)2$ does not simply track the edge of the beam footprint, where $F\rightarrow 0$ J/cm2, but rather is determined by a threshold lifetime value of the film material. The reasons to expect the ablation boundaries of a damage site to be closely co-located with the threshold damage are explained as follows. First, the Gaussian beam and resulting steep temperature profile decrease rapidly with r beyond the beam axis; thus, the threshold fluence is quickly reached past the ablation line. Specifically, film damage and ablation processes are thermally activated; thus, the onset of damage is exponentially (Arrhenius) dependent providing a sharp transition line. Second, the thresholding imaging analysis does not distinguish specifically the ablation area, and it can also include any damage-affected areas beyond the ablation line depending on the imaging and analysis sensitivity. Further, for short nanosecond pulse lengths, the in-plane thermal diffusion is very limited (<100 nm), compared to the size of the damage considered and the beam diameter ($2w0$=94 μm). Still, even in the non-ablative regime, Fprobe can be determined, in principle, by the extrapolation method in Fig. 2A using imaging of other apparent damage modes, such as film darkening, thinning, or melting [14].

Lifetime damage threshold values, $F\text{th}(N)$, are calculated using Eq. (1) with $R\text{th}(N)$ measurements derived from $N\times F$probe exposures [Fig. 2B] and $w0$ derived as the slope of the fitted data in Fig. 2A. The results are shown in Fig. 2C for a representative test on a 20 nm thick gold film on sapphire substrate. The $F\text{th}(N)$ values saturates for $N>\sim 100$ exposures, which suggests that at this fluence $F\text{th}(\text{DSA},N>100)=0.41$ J/cm2 or less, the film will not damage for any number of exposures. This DSA threshold value matches that determined from the $S(N=100)/1$ method $F\text{th}(S(N)/1,N=100)=0.40J$/cm2 on the same film [Fig. 2D]. To extract the DSA and $S/1F\text{th}$ values in Figs. 2C and 2D, respectively, the data were fitted (solid lines) to semi-empirical expressions described previously [19]. Only a single fixed fluence, Fprobe, is necessary to determine that $F\text{th}(N)$ as the number of exposures was increased to reach damage size saturation for $N>100$ [Figs. 2B and 2C]. In other studies, both the input fluence and N are varied to derive lifetime damage thresholds, necessitating a far greater number of exposures and data analysis [11,20–23]. In contrast, once Fprobe is determined, the DSA method takes advantage of the fluence contrast within the beam profile to probe a range of fluence levels simultaneously. It is not obvious, *a priori*, that this approach should be effective in determining a threshold since dynamic effects may affect the location of the damage site boundary. In addition, Fprobe, based on a single exposure ablation threshold was selected here for convenience. However, the incubation behavior at this fluence, whereby film absorption and damage increase with repeated exposures, may result in $(2R\text{th}(N))2$ saturating at the $\sim(2w0)2$ value, rather than at a threshold fluence value. These considerations are likely to be material and laser parameter dependent; thus, more data are necessary to fully address whether an $F\text{probe}(N=1)$ based on a near-ablation threshold is ideal for lifetime damage measurements.

To validate the DSA method, additional film material systems were tested, including oxides, metal, and graphene, and films prepared on sapphire (Al2O3) and fused silica (FS) substrates to address the broad applicability of the DSA method. The results are compared directly with the established results from the $S(N=100)/1$ test method in Fig. 3, where the threshold values are

extracted using reported semi-empirical fits of the Fth(N) and probability curve data in Figs. 2C and 2D [19]. The Fth(N=100) thresholds are plotted for the DSA method (y-axis) and for the S(N=100)/1 method plotted on the x-axis. Perfect agreement where Fth(DSA)=Fth(S(N)/1 is shown as the dashed line for reference. The solid line represents a linear fit of the data showing the two methods produce nearly identical thresholds, although the slope is slightly below unity ~0.97. Still, this result confirms that the DSA is an efficient alternative for deriving lifetime optical damage thresholds on a broad range of film materials. An estimate of the Fth error from DSA can be derived based on the experimental Fprobe percent error (estimated at ±3%), n, and Eq. (1) by multiplying the right-hand side of Eq. (1) by (1±n/100) and solving for the relative error, which results in a maximum error in Fth of $-n/(100+n)F$th and $+n/(100-n)F$th. Thus, Fth±error bars in Fig. 3 are −2.9% and 3.1% of Fth

.

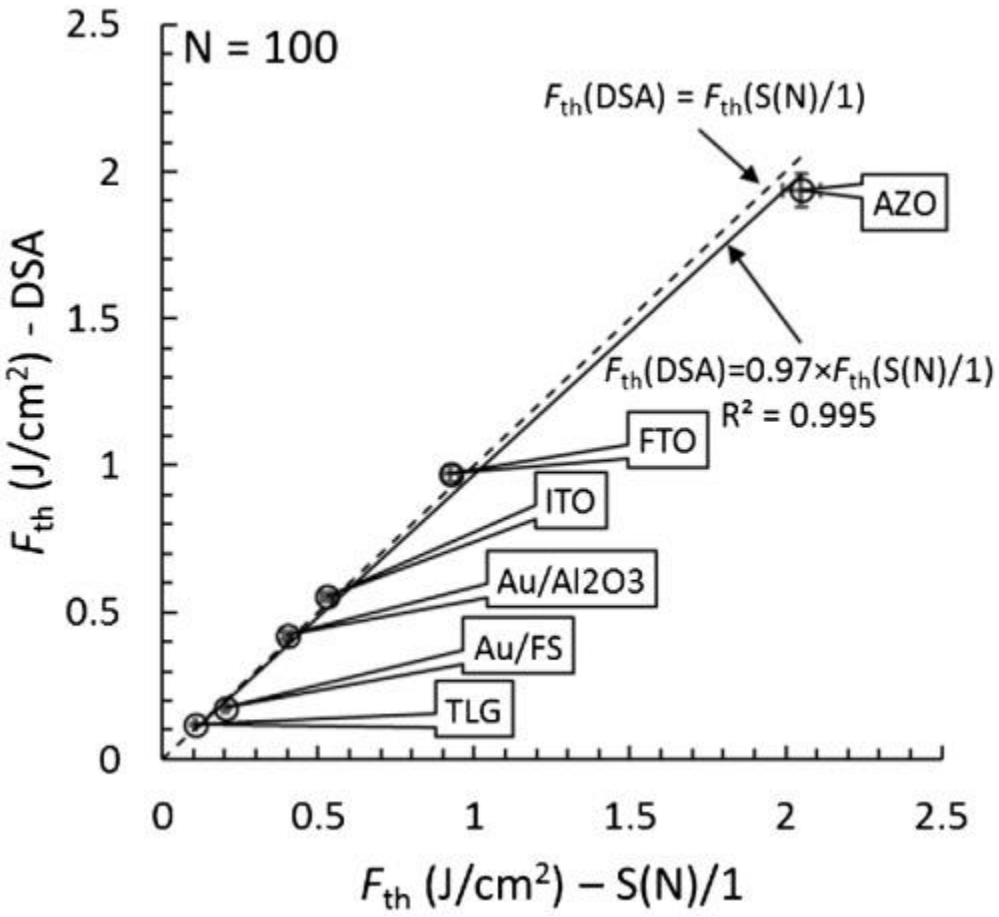

Fig. 3. Comparison of lifetime optical damage thresholds derive from the DSA damage test method and the S(N)/1 method. Error bars on S(N)/1 Fth values are taken as the ±3% laser power stability, while DSA Fth error were calculated as discussed in text.

For materials where distributed small defect absorption drives localized laser damage, the damage location is less deterministic, and the damage size can be decoupled from the beam

fluence profile. In this case, the DSA method may become unsuitable unless the lowest threshold absorbing defect density and the resulting spacing between the damage spots are much smaller than the laser exposure area [14,19]. For film materials where damage results from bulk absorption processes, the DSA method should be broadly applicable, even to bulk material surfaces such as metals, plasmonic materials, metal oxides, polymers, and biological samples.

The DSA method presented here extends single-shot threshold measurements [18] to the important problem of lifetime (multi-shot) damage threshold determination which is the relevant design parameter in repetition-rated, high-power lasers and optoelectronic devices. A single exposure evaluation significantly overestimates the material threshold due to the incubation effect. For improved accuracy, the analysis and extraction of the lifetime threshold values are based on a semi-empirical fitting of lifetime incubation data [19]. We also introduced a systematically selected probe fluence (Fprobe) to test the lifetime optical damage performance, making the procedure more reproducible, reliable, and amenable to automation. The DSA approach was tested across a range of material systems for validation by direct comparison with the S/1 reference damage test method. The DSA method can implement the same ISO standard requirements as the S/1 method for site spacing, exposure numbers, imaging, and analysis to extract a lifetime damage threshold value [24]. Still, the beam profile and probe fluence (Fprobe) would need to be added as new requirements. Finally, the DSA efficiency gains (processing time, sample area, analysis), in principle, could be further increased by monitoring *in situ* a single test site damage size versus N, instead of using different sites for each number of N exposures tested.

Funding

U.S. Department of Energy (DOE) (15-ERD-057, DE-AC52-07NA27344).

Acknowledgment

The work in this Letter was performed under the auspices of the U.S. Department of Energy by Lawrence Livermore National Laboratory within the LDRD program.

REFERENCES

1. J. Y. Natoli, L. Gallais, H. Akhouayri, and C. Amra, Appl. Opt. **41**, 3156 (2002). [CrossRef]

2. A. Bayramian, J. Armstrong, G. Beer, R. Campbell, B. Chai, R. Cross, A. Erlandson, Y. Fei, B. Freitas, R. Kent, J. Menapace, W. Molander, K. Schaffers, C. Siders, S. Sutton, J. Tassano, S. Telford, C. Ebbers, J. Caird, and C. Barty, J. Opt. Soc. Am. B **25**, B57 (2008). [CrossRef]

3. J. J. Adams, J. A. Jarboe, M. D. Feit, and R. P. Hackel, Proc. SPIE **6720**, 72014 (2008).

4. S. Schrameyer, M. Jupe, L. Jensen, and D. Ristau, Proc. SPIE **8885**, 88851J (2013). [CrossRef]

5. Z. M. Liao, M. L. Spaeth, K. Manes, J. J. Adams, and C. W. Carr, Opt. Lett. **35**, 2538 (2010).

6. D. A. Cross and C. W. Carr, Appl. Opt. **50**, D7 (2011). [CrossRef]

7. M. C. Nostrand, T. L. Weiland, R. L. Luthi, J. L. Vickers, W. D. Sell, J. A. Stanley, J. Honig, J. Auerbach, R. P. Hackel, and P. J. Wegner, Proc. SPIE **5273**, 325 (2003). [CrossRef]

8. D. A. Alessi, C. W. Carr, R. P. Hackel, R. A. Negres, K. Stanion, J. E. Fair, D. A. Cross, J. Nissen, R. Luthi, G. Guss, J. A. Britten, W. H. Gourdin, and C. Haefner, Opt. Express **23**, 15532 (2015). [CrossRef]

9. K. Soong, R. L. Byer, E. R. Colby, R. J. England, and E. A. Peralta, AIP Conf. Proc. **1507**, 511 (2012).

10. A. Ben-Yakar and R. L. Byer, J. Appl. Phys. **96**, 5316 (2004). [CrossRef]

11. M. Lenzner, Z. L. Sun, and W. Rudolph, Proc. SPIE **9237**, 923714 (2014). [CrossRef]

12. J. M. Liu, Opt. Lett. **7**, 196 (1982). [CrossRef]

13. I. L. Bass, R. A. Negres, K. Stanion, G. Guss, and J. Bude, Appl. Opt. **55**, 3131 (2016). [CrossRef]

14. J.-H. Yoo, M. G. Menor, J. J. Adams, R. N. Raman, J. R. I. Lee, T. Y. Olson, N. Shen, J. Suh, S. G. Demos, J. Bude, and S. Elhadj, Opt. Express **24**, 17616 (2016). [CrossRef]

15. https://doi.org/10.6084/m9.figshare.5187883.

16. https://doi.org/10.6084/m9.figshare.5187886.

17. https://doi.org/10.6084/m9.figshare.5187889.

18. M. Sozet, J. Neauport, E. Lavastre, N. Roquin, L. Gallais, and L. Lamaignere, Opt. Lett. **41**, 804 (2016). [CrossRef]

19. S. Elhadj, J.-H. Yoo, R. A. Negres, M. G. Menor, J. J. Adams, N. Shen, D. A. Cross, I. L. Bass, and J. D. Bude, Opt. Mater. Express **7**, 202 (2017). [CrossRef]

20. S. Z. Xiao, E. L. Gurevich, and A. Ostendorf, Appl. Phys. A **107**, 333 (2012). [CrossRef]

21. G. Raciukaitis, M. Brikas, P. Gecys, and M. Gedvilas, Proc. SPIE **7005**, 70052L (2008). [CrossRef]

22. Z. L. Sun, M. Lenzner, and W. Rudolph, J. Appl. Phys. **117**, 073102 (2015). [CrossRef]

23. D. Ashkenasi, M. Lorenz, R. Stoian, and A. Rosenfeld, Appl. Surf. Sci. **150**, 101 (1999). [CrossRef]

24. “Lasers and laser-related equipment—Test methods for laser-induced damage threshold—Part 1: Definitions and general principles,” ISO 21254-1:2011 (2011).